POLISH JOURNAL *of* RADIOLOGY

Original paper

Texture analysis on routine MRI sequences to differentiate between focal nodular hyperplasia and hepatocellular adenoma

Faeze Salahshour[1,2,A,E], Afshar Ghamari Khameneh[1,B,C,D,E,F], Gisoo Darban Hosseini Amirkhiz[1,B,D], Niloofar Ayoobi Yazdi[1,2,A,B], Sajad Shafiekhani[3,B,D]

[1]Department of Radiology, Advanced Diagnostic and Interventional Radiology (ADIR) Research Center, Imam Khomeini Hospital Complex, Tehran University of Medical Sciences, Tehran, Iran
[2]Liver Transplantation Research Center, Imam-Khomeini Hospital, Tehran University of Medical Sciences, Tehran, Iran
[3]Department of Biomedical Engineering, School of Medicine, Tehran University of Medical Sciences, Tehran, Iran

Abstract

Purpose: We investigated the diagnostic power of texture analysis (TA) performed on MRI (T2-weighted, gadolinium-enhanced, and diffusion-weighted images) to differentiate between focal nodular hyperplasia (FNH) and hepatocellular adenoma (HCA).

Material and methods: This was a retrospective single-centre study. Patients referred for liver lesion characterization, who had a definitive pathological diagnosis, were included. MRI images were taken by a 3-Tesla scanner. The values of TA parameters were obtained using the ImageJ platform by an observer blinded to the clinical and pathology judgments. A non-parametric Mann-Whitney U test was applied to compare parameters between the 2 groups. With receiver operating characteristic (ROC) analysis, the area under the curve (AUC), sensitivity, and specificity were calculated. Finally, we performed a binary logistic regression analysis. A p-value <0.05 was reported as statistically significant.

Results: A total of 62 patients with 106 lesions were enrolled. T2 hyperintensity, Atoll sign, and intralesional fat were encountered more in HCAs, and central scars were more frequent in FNHs. Multiple TA features showed statistically significant differences between FNHs and HCAs, including skewness on T2W and entropy on all sequences. Skewness on T2W revealed the most significant AUC (0.841, good, $p < 0.0001$). The resultant model from binary logistic regression was statistically significant ($p < 0.0001$) and correctly predicted 84.1% of lesions. The corresponding AUC was 0.942 (excellent, 95% CI: 0.892-0.992, $p < 0.0001$).

Conclusion: Multiple first-order TA parameters significantly differ between these lesions and have almost fair to good diagnostic power. They have differentiation potential and can add diagnostic value to routine MRI evaluations.

Key words: focal nodular hyperplasia, adenoma, hepatocellular, magnetic resonance imaging.

Introduction

After haemangiomas, focal nodular hyperplasia (FNH) and hepatocellular adenoma (HCA) are the second and third most common benign liver tumours, respectively, which traditionally involve young to middle-aged women [1].

They share similar radiologic traits but have different management and prognoses. HCAs carry a risk of fortuitous bleeding and progression to malignant transformation, while complications of FNHs are scarce (do-not-touch lesion) [1,2]. The best non-invasive diagnostic method is imaging, but each modality has some limita-

tions. For instance, a multiphasic computed tomography (CT) scan often comes into play as an initial modality. However, in the absence of characteristic findings such as a central scar or discoverable fat inside the lesion, the diagnosis is problematic [3]. Magnetic resonance imaging (MRI) is the most chosen tactic for characterizing focal liver lesions [4,5]. A sensitivity of 60-70% and a specificity close to 100% for FNH expected when MRI depicts the established characteristic features such as a central scar, marked arterial hyperenhancement, and lobulated contours. Unfortunately, around 50% of FNHs show typical findings, and in many cases, the distinction between FNH and HCA is not achievable [6]. There is also the possibility of findings overlapping in hyper-enhancing liver lesions in the arterial phase [7]. In such cases, either liver biopsy, an invasive method, or Gadoxetic acid-enhanced magnetic resonance imaging (GAE-MRI) should be used [8]. In GAE-MRI, despite the high sensitivity and specificity (hypointense in the hepatobiliary phase), HCA in the hepatobiliary phase is iso- to hyperintense in 7-26% of cases [9-11]. Conversely, 3-8% of FNH are hypointense in the phase mentioned earlier [10,11]. In addition, the Gadoxetic acid contrast agent is unavailable in middle-low-income countries. As a result, it is necessary to find an alternative method to improve the diagnosis, and reduce the cost and risk of invasiveness [11-14].

Texture analysis (TA) is an old-established mathematical method in which the heterogeneity of the lesion is characterized based on the distribution of pixel intensities in the range of the desired mode [15]. TA can detect subtle changes that are visually indistinguishable. In the liver, it is used to distinguish malignant from benign lesions [16,17], the correlation between imaging, molecular and histopathological findings of tumour [18], evaluation of prognosis, and response to treatment in patients with hepatocellular carcinoma (HCC) and liver metastases [19-21]. Different methods of TA are available, but the most common form is first-order statistics. A histogram derived from grey levels of pixel intensities and multiple parameters can be calculated, including mean, standard deviation, skewness, kurtosis, and entropy [22]. Compared to a CT scan, MRI gives higher contrast of soft tissues, and TA derived from MRI is more effective in reflecting the tumour heterogenicity [16,22].

In this study, we aim to investigate the diagnostic power of TA performed on MRI with common sequences (T2-weighted, gadolinium-enhanced, and diffusion-weighted images [DWI]) to differentiate HCA from FNH.

Material and methods

Population, ethics, and confirmation

The investigated population includes patients who were referred to our hospital for characterization of liver lesions between 2014 and 2022 and had a definitive pathological

or radiological diagnosis of HCA or FNH. The study's nature was retrospective and observational, and its code of ethics is IR.TUMS.IKHC.REC.1400.250 (Tehran University of Medical Sciences, Imam Khomeini Hospital Complex). The study was conducted according to established ethical guidelines and regulations. Written informed consent was obtained. Patients' information was entered into the study in a confidential and coded manner. Informed consent was obtained from the patients for the publication of their images. The principles of the Declaration of Helsinki were observed.

To be included in this study, patients had to be 18 years old or above and undergo an MRI with extracellular contrast agent (gadolinium) and/or DWI within 6 months before surgery or biopsy. Exclusion criteria were poor quality of images, unclear margins of lesions, suboptimal arterial phase, presence of bleeding or necrosis within the lesion based on imaging findings (increased or heterogeneous T1 for bleeding and high T2 for necrosis), damaged or lost source file within the database, and small size of the lesions (diameter < 5 mm or ROI < 100 pixels).

The gold standard of final diagnosis is the confirmation of pathology obtained from core needle biopsy samples or surgical resection [23].

MRI technique, lesion selection, and texture analysis

MRI images were taken by a 3-Tesla scanner (Magnetom Trio®, Siemens Healthcare, Erlangen, Germany) with axial directed fast spin-echo T2-weighted, gradient recalled echo T1-weighted with fat saturation, single shot breath holding echo planar DWI. An ADC map was generated at high (800 s/mm²) b-values. Gadolinium (Gd-DTPA, Kangchen Pharmaceutical Company Ltd., Guangzhou, China) was used with a fast bolus injection (0.2 mmol/kg) followed by a 20 ml 0.9% saline chaser, both with a 20 ml/sec rate. Dynamic images were taken every 15-20 seconds after contrast medium injection. Arterial and portal phases were acquired 20-40 and 60-70 seconds after injection, respectively (Table 1).

Demographic information such as age and gender were extracted from the files. MR images were extracted from PACS (Picture Archive and Communication System database) in the bitmap format. Qualitative features on MRI were considered as follows: arterial hyperenhancement lesion signal intensity more than surrounding liver parenchyma in the arterial phase; significant T2 hyperintensity the signal intensity similar or more than the spleen on T2 signals; atoll sign, a peripheral rim of high intensity with central lesion iso intensity on T2; intralesional fat, at least 20% drop of signal intensity on opposed-phase of gradient echo images in comparison with in-phased images; central scar, star-like structure with T2 hyperintensity and arterial and portal hypo enhancement and delayed hyperenhancement at the centre of the lesions.

Table 1. Acquisition technique

Sequence	TE (ms)	TR (ms)	ST (mm)	Gap/Space (mm)	Matrix	FOV (mm)	FAº
T2-weighted	80-99	508-891	5	2.5	320 × 192	380 × 380	90
Contrast-enhanced (arterial/portal)	2	4	4	2	256 × 192	400 × 400	12
DWI	69-76	5300-9474	6-8	5-9	82 × 82	400 × 400	90

TE – time of echo, TR – time of repetition, ST – slice thickness, FOV – field of view, FA – flip angle, DWI –diffusion-weighted image.

The values of TA parameters were obtained by the ImageJ free platform (National Institutes of Health, Bethesda, MD, USA) by an observer blinded to the clinical and pathology judgments. A polygonal ROI (region of interest) was drawn manually in the largest cross-sectional diameter (2D slices) within the margins of the lesions at the same position in different sequences (Figure 1). Skewness (asymmetry of the pixel distribution), kurtosis (tailedness of the pixel distribution), and entropy (measure of irregularity or randomness) were obtained. The mentioned TA parameters derived from unfiltered images and were not sensitive to the scan protocols [22,24]. The pixel intensity ranged from 0 to 255.

Statistical analysis

Continuous quantitative data were reported as mean ± standard deviation, and qualitative data were reported as numbers and percentages. To compare parameters between the 2 groups, initially, the normality of data distribution was checked by the Kolmogorov-Smirnov test, and then a non-parametric Mann-Whitney U test was applied for comparisons. The χ^2 test was performed for the comparison of categorical variables. With receiver operating characteristic (ROC) analysis, the area under the curve (AUC), sensitivity, and specificity of each parameter were calculated. The diagnostic power of the test was classified as follows [25]: 0.9-1: excellent; 0.8-0.9: good; 0.7-0.8: fair; 0.6-0.7: poor; 0.5-0.6: fail. In the final step, a binary logistic regression was performed, including statistically significant features.

A measured p-value <0.05 was reported as statistically significant. Statistical analyses were performed by IBM SPSS version 25 software.

Results

Study population

A total of 62 patients, including 57 women and 5 men, were included in this study. The age of the patients was between 18 and 59 years, with an average of 35.63 and a standard deviation of 9.62. Of these patients, 106 lesions were included in this investigation. Fifty lesions were FNH, and 56 were liver adenomas. The selection process and excluded cases are exhibited in Figure 2.
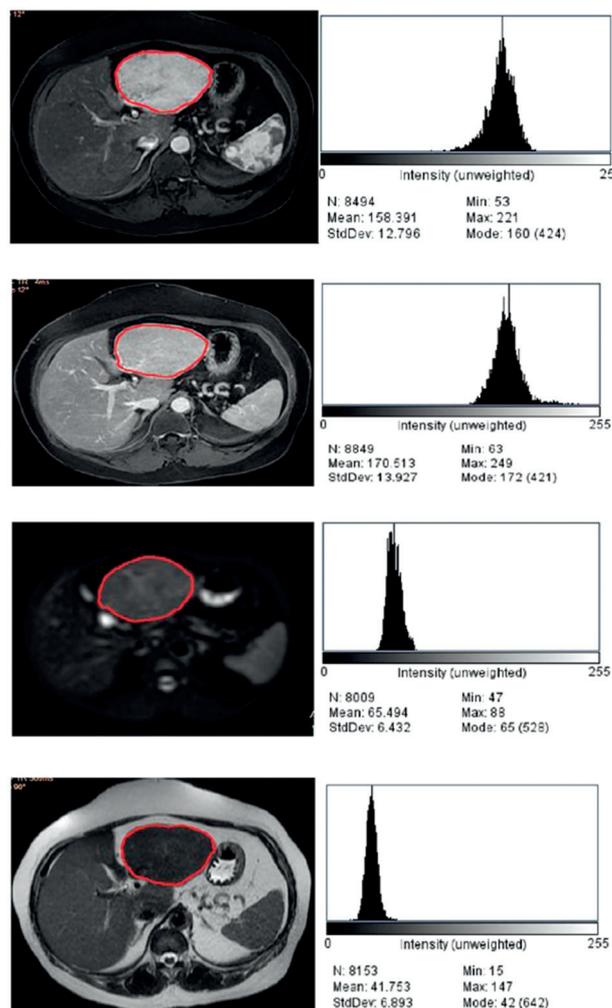

Figure 1. Lesion selection and the histogram diagram resulting from the distribution of the pixels. The margin of the mass marked with a red marker. From top to bottom, images on the right side related to arterial, portal, DWI, and T2-weighted sequences. The histogram derived from each lesion is shown on the left side of the corresponding sequences

Moderate to strong arterial hyperenhancement was found in 49 FNHs and 55 HCAs, which was not statistically significant. On the other hand, T2 hyperintensity (2 vs. 27), atoll sign (0 vs. 16), and intralesional fat (2 vs. 13) were more often encountered in HCAs, and central scars (48 vs. 16) were more frequent in FNHs. The largest AUC (77.7, fair) was attributed to the central scar (sensitivity: 84%; specificity: 71.4%). The length and qualitative characteristics of lesions are shown in Table 2.
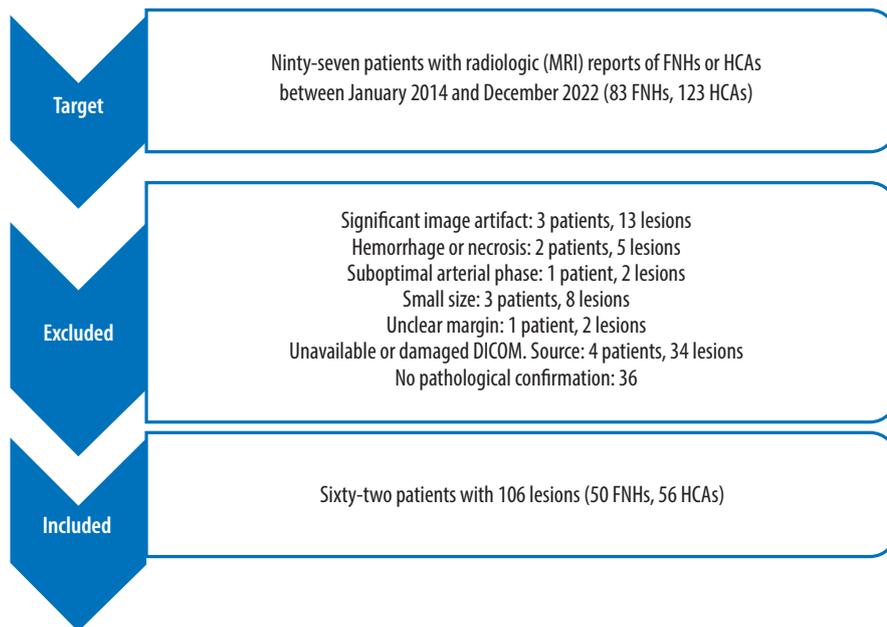
Figure 2. The selection process and final population presented in this flow diagram. FNH: focal nodular hyperplasia, HCA: hepatocellular adenoma

Table 2. Qualitative features of liver MRI of focal nodular hyperplasia and hepatocellular adenoma

Characteristics		Focal nodular hyperplasia (*n*=50)	Hepatocellular adenoma (*n*=56)	*p*-value*
Moderate to marked enhancement on the arterial phase	Present	49	55	0.935
	Absent	1	1	
T2 hyperintensity	Present	2	27	< 0.001
	Absent	48	29	
Atoll sign	Present	0	16	< 0.001
	Absent	50	40	
Intralesional fat	Present	2	13	0.005
	Absent	48	43	
Central scar	Present	42	16	< 0.001
	Absent	8	40	

*χ^2 test

Texture analysis

Multiple TA features showed statistically significant differences between FNHs and HCAs. In the T2W sequence, the mean value of skewness (0.38 ± 0.34, −0.17 ± 0.28, $p < 0.0001$) and entropy (3.80 ± 0.39, 3.25 ± 0.41, $p < 0.001$) of FNHs were higher than those of HCAs. The mean value of entropy in the arterial phase (4.64 ± 0.49, 4.28 ± 0.57, $p = 0.001$), portal phase (4.28 ± 0.55, 4 ± 0.54, $p = 0.018$), and DWI (4.1 ± 0.6, 3.68 ± 0.67, $p = 0.005$) were also statistically different between the 2 groups. Details of these comparisons are shown in Table 3.

Skewness on T2 revealed the most significant AUC on ROC analysis (0.841, good, $p < 0.0001$) (Figure 3). A value of less than −0.04 has a sensitivity of 96.7% and a specificity

of 66.7% for diagnosing HCAs. Entropy on the DWI (AUC: 0.808, $p < 0.0001$) also showed good performance. Entropy on arterial and portal phase and T2W presented fair diagnostic power. Diagnostic performance is reported in Table 4.

Logistic regression analysis

A binary logistic regression analysis carried out using the diagnosis as the dependent variable and the following covariates: atoll sign, intralesional fat, central scars, T2 hyperintensity, skewness on T2W images, and entropy on arterial phase, portal phase, DWI, and T2W. The resultant model was statistically significant ($p < 0.0001$) and correctly predicted 84.1% of lesions. The corresponding AUC was 0.942, i.e. excellent ($p < 0.0001$) (Figure 4).

Table 3. Texture analysis of liver MRI of focal nodular hyperplasia and hepatocellular adenoma

Textural analysis		Diagnosis	Minimum	Maximum	Mean	Std. deviation	*p*-value*
T2-weighted images	Skewness	FNH	−0.5	0.95	0.38	0.34	< 0.001
		Adenoma	−0.9	0.22	−0.17	0.28	
	Kurtosis	FNH	−1.13	0.9	−0.10	0.49	0.880
		Adenoma	−1.08	1.08	−0.10	0.46	
	Entropy	FNH	3.22	4.68	3.80	0.39	< 0.001
		Adenoma	2.29	3.83	3.25	0.41	
Arterial phase	Skewness	FNH	−1.02	0.48	−0.24	0.40	0.439
		Adenoma	−1.22	0.71	−0.30	0.42	
	Kurtosis	FNH	−0.94	1.79	0.03	0.74	0.870
		Adenoma	−1.17	1.39	0.01	0.68	
	Entropy	FNH	3.43	5.79	4.64	0.49	0.001
		Adenoma	3.13	5.42	4.28	0.57	
Portal phase	Skewness	FNH	−1	1.18	0.08	0.46	0.214
		Adenoma	−0.97	1.1	−0.02	0.45	
	Kurtosis	FNH	−1.18	1.09	0.1	0.57	0.979
		Adenoma	−1.06	1.18	−0.09	0.58	
	Entropy	FNH	3.25	5.48	4.28	0.55	0.018
		Adenoma	2.65	5.10	4	0.54	
Diffusion-weighted images	Skewness	FNH	−1.34	0.98	−0.02	0.45	0.459
		Adenoma	−1.07	1.02	0.05	0.50	
	Kurtosis	FNH	−1.12	0.71	−0.25	0.52	0.466
		Adenoma	−1.01	1	−0.17	0.48	
	Entropy	FNH	3.06	5.64	4.10	0.60	0.005
		Adenoma	2.62	4.94	3.68	0.67	

*Mann-Whitney *U* test, FNH – focal nodular hyperplasia, HCA – hepatocellular adenoma

Discussions

In our investigation of distinguishing FNHs from HCAs, the skewness on the T2W sequence and entropy on all sequences had statistically significant different distributions. All these parameters were higher in FNHs. The diagnostic performance was almost fair to good, with AUC values ranging from 0.743 (entropy on portal phase) to 0.841 (skewness on T2W). The central scar was the best traditional finding for differentiation (AUC: 77.7), but as we said, TA parameters can show better overall diagnostic power. Furthermore, our final model consists of all significant features with outstanding performance (AUC: 0.942, sensitivity: 88.5%, specificity: 83.7%). Eighty-four per cent of lesions were correctly predicted. So, we believe that first-order TA derived from liver MRI is a simple, fast, reliable, and non-invasive ancillary or complementary tool for distinguishing these lesions. They successfully reflected the histopathological heterogenicity in our study.

Despite low availability and no guarantee of the superiority of texture analysis based on MRI images with hepatobiliary contrast agent (in comparison with extra-
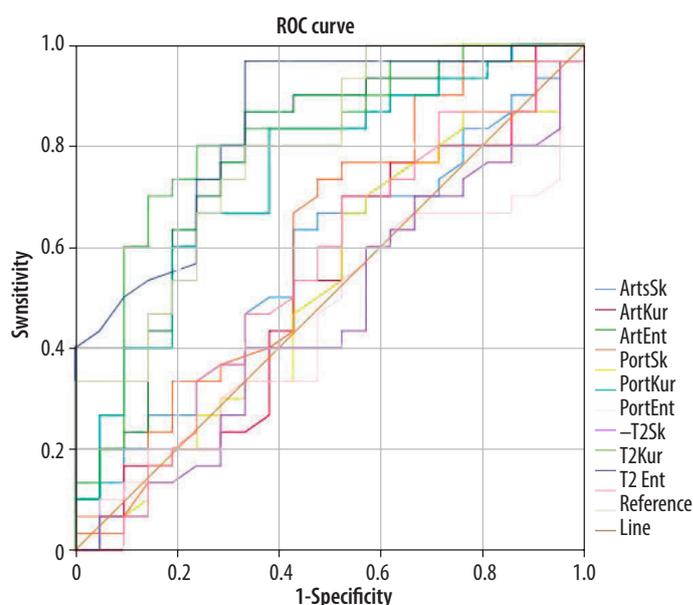
Figure 3. ROC curves of texture analysis parameters. ArtsSk – arterial skewness, ArtKur – arterial kurtosis, ArtEnt – arterial entropy,; PortSk – portal skewness, PortKur – portal kurtosis, PortEnt – portal entropy, T2Sk – T2 skewness, T2Kur – T2 kurtosis, T2 Ent – T2 entropy

Table 4. Diagnostic performance of texture analysis

Parameters	AUC* (95% CI)	*p*-value	Optimal cut-off**	Sensitivity (%)	Specificity (%)
Skewness on T2-weighted images	0.841 (0.73-0.952)	< 0.0001	≤ −0.04	96.7	66.7
Entropy on diffusion-weighted images	0.808 (0.682-0.934)	< 0.0001	≤ 3.75	80	76.2
Entropy on T2-weighted images	0.787 (0.66-0.914)	0.001	< 3.38	80	66.7
Entropy on arterial phase	0.768 (0.628-0.909)	0.001	< 4.35	86.7	66.7
Entropy on portal phase	0.743 (0.604-0.882)	0.003	< 3.90	83.3	61.9

*ROC analysis, **Youden Index
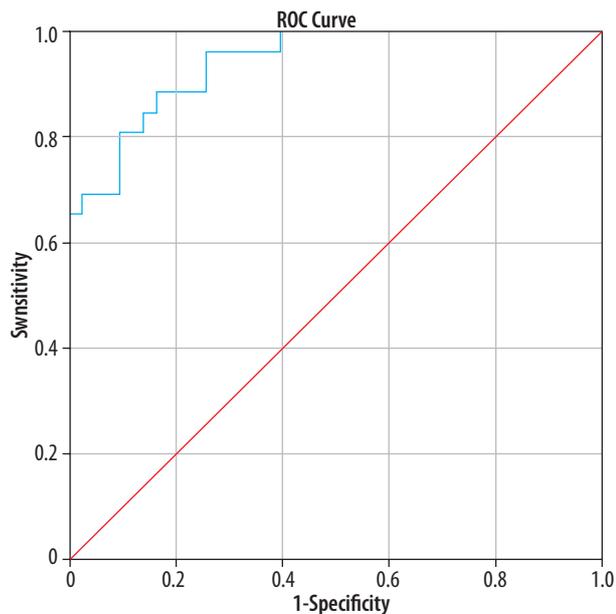
Figure 4. ROC curve of predicted probabilities of model for diagnosis of hepatocellular adenoma. The model consisted of atoll sign, intralesional fat, central scars, T2 hyperintensity, skewness on T2-weighted images, entropy on T2-weighted images, diffusion weighted images, and arterial and portal phases

cellular contrast agent), studies designed to distinguish HCAs from FNHs are predominantly based on them and CT scans. So far, no study used the identical MRI sequences as in our investigation for comparison. In the study of Canella *et al.*, 51 HCAs from 40 patients and 32 FNHs from 28 patients underwent GAE-MRI. TA on T2 fast spin-echo sequences, hepatic arterial, and hepatobiliary phases were assessed. Among different texture parameters, skewness in the T2-weighted, arterial phase, and hepatobiliary phase, as well as entropy in the hepatobiliary phase, had another distribution, which was statistically significant. The highest AUC (0.87) was related to skewness in the hepatobiliary phase. By adding TA parameters to the main criteria of hypointensity in the hepatobiliary phase, the AUC for the HCA diagnosis reached 0.98. In fact, with this method, 96.4% of lesions were correctly identified. As a result, TA has an added value for detecting atypical HCAs that do not show hypointensity in the hepatobiliary phase [26]. The TA based on T2W in this study almost followed our investigation. They calculated

that the mean skewness on T2W was higher in FNHs (0.91 ± 0.84 vs. 0.21 ± 0.56, *p* < 0.001). Their mentioned optimal cut-off was less than 0.18, with sensitivity 58.8% and specificity 87.5%.

There are some other studies in the literature showing that TA of liver MRI is helpful for the discrimination of different histopathological lesions. For instance, the following 3 works were designed to focus on texture analysis based on the T2W sequence. First, in the study of Zhong *et al.*, 68 patients with 73 liver nodules (46 HCCs and 27 dysplastic nodules, confirmed by pathology) were examined. The diagnostic power of GAE-MRI, DWI, the combination of these 2 modalities, and TA based on T2-weighted images was investigated. To distinguish small HCC from dysplastic nodules, the AUC in TA was 0.96, which was significantly higher than both types of GAE-MRI (0.86) and DWI alone (0.8). Meanwhile, a combination of these 2 imaging modalities showed almost identical sensitivity (95.6% vs. 97.8%), but the specificity declined notably (66.7% vs. 92.6%) in comparison with TA [27]. Second, Stocker *et al.* reviewed the preoperative contrast-enhanced MRI (native fat-saturated T1W, T2W, and arterial and portal phase) of 108 non-cirrhotic patients retrospectively. TA was performed by 2 separate readers, comparing the grey-level histogram, co-occurrence, and run-length matrix with 19 parameters. Two radiologists reviewed the images. The diagnostic power of TA was compared with the routine radiological examination. Their results showed that texture analysis of routine liver MRI effectively distinguished the masses mentioned above [28]. Finally, in the study by Li *et al.*, TA findings from spectral attenuated inversion-recovery T2-weighted MRI (SPAIR T2W-MRI) of a total of 162 patients (55 haemangiomas, 67 liver metastasis, and 40 HCCs) were reviewed retrospectively. TA parameters were calculated from the grey-level co-occurrence matrix, grey-level gradient co-occurrence matrix, grey-level run-length matrix, Gabor wavelet transform, and intensity-size-zone matrix. They claimed that TA findings obtained from SPAIR T2W-MRI for the diagnosis of single liver lesions can be used as an ancillary tool for more accurate diagnosis. However, none of the parameters is useful alone (a combination of 9 to 16 parameters must be used) [16]. To sum up, all the mentioned works confirm that TA can be helpful in diagnostic

challenges of liver lesions, either benign or malignant, so it deserves special attention. Our results are in accordance with the mentioned studies, and TA based on the T2W sequence reflects the histopathological difference.

The first limitation of our study was that it was conducted retrospectively over 8 years, which may affect the homogeneity of the image acquisition technique. However, previous studies have shown that the TA parameters used in our work are not significantly affected because the mean, standard deviation, and mean positive pixels (MPP) may be involved [24]. Also, larger multicentre prospective studies are suggested, to verify the practicality and generality. Our analysis was performed in the largest cross-sectional area in 2D, and a survey in 3D is strongly recommended (considering all parts of a lesion). The T1-weighted and delayed phase were not investigated because masses are isointense on these sequences, and they rarely provide sufficient contrast. It must be noted that the volume and the concentration of contrast medium influence the TA [22], but the type (hepatobiliary vs. gadolinium) was not investigated.

Conclusions

Accurate non-invasive diagnosis plays a vital role in managing FNH and HCA. First-order TA parameters on the T2W sequence (skewness and entropy), DWI (entropy), portal (entropy), and arterial phase (entropy) significantly differ between these lesions and have almost fair to good diagnostic power. They have differentiation potential and can add diagnostic value to routine MRI evaluations.

Conflict of interest

The authors report no conflict of interest.

References

1. Nault JC, Couchy G, Balabaud C, et al. Molecular classification of hepatocellular adenoma associates with risk factors, bleeding, and malignant transformation. Gastroenterology 2017; 152: 880-894.e6. doi: 10.1053/j.gastro.2016.11.042.

2. Navarro AP, Gomez D, Lamb CM, et al. Focal nodular hyperplasia: a review of current indications for and outcomes of hepatic resection. HPB (Oxford) 2014; 16: 503-511.

3. Ruppert-Kohlmayr AJ, Uggowitzer MM, Kugler C, et al. Focal nodular hyperplasia and hepatocellular adenoma of the liver: differentiation with multiphasic helical CT. AJR Am J Roentgenol 2001; 176: 1493-1498.

4. Vilgrain V. Focal nodular hyperplasia. Eur J Radiol 2006; 58: 236-245.

5. Marin D, Brancatelli G, Federle MP, et al. Focal nodular hyperplasia: typical and atypical MRI findings with emphasis on the use of contrast media. Clin Radiol 2008; 63: 577-585.

6. Cogley JR, Miller FH. MR imaging of benign focal liver lesions. Radiol Clin North Am 2014; 52: 657-682.

7. Agarwal S, Fuentes-Orrego JM, Arnason T, et al. Inflammatory hepatocellular adenomas can mimic focal nodular hyperplasia on Gadoxetic acid-enhanced MRI. Am J Roentgenol 2014; 203: W408-W414. doi: 10.2214/AJR.13.12251.

8. Cannella R, Borhani AA, Minervini MI, et al. Evaluation of texture analysis for the differential diagnosis of focal nodular hyperplasia from hepatocellular adenoma on contrast-enhanced CT images. Abdom Radiol (NY) 2019; 44: 1323-1330.

9. Glockner JF, Lee CU, Mounajjed T. Inflammatory hepatic adenomas: Characterization with hepatobiliary MRI contrast agents. Magn Reson Imaging 2018; 47: 103-110.

10. Grieser C, Steffen IG, Kramme IB, et al. Gadoxetic acid enhanced MRI for differentiation of FNH and HCA: a single centre experience. Eur Radiol 2014; 24: 1339-1348.

11. Grazioli L, Bondioni MP, Haradome H, et al. Hepatocellular adenoma and focal nodular hyperplasia: value of Gadoxetic acid-enhanced MR imaging in differential diagnosis. Radiology 2012; 262: 520-529.

12. An HS, Park HS, Kim YJ, et al. Focal nodular hyperplasia: characterisation at Gadoxetic acid-enhanced MRI and diffusion-weighted MRI. Br J Radiol 2013; 86: 20130299. doi: 10.1259/bjr.20130299.

13. Zech CJ, Grazioli L, Breuer J, et al. Diagnostic performance and description of morphological features of focal nodular hyperplasia in Gd-EOB-DTPA-enhanced liver magnetic resonance imaging: results of a multicenter trial. Invest Radiol 2008; 43: 504-511.

14. Grazioli L, Morana G, Kirchin MA, Schneider G. Accurate differentiation of focal nodular hyperplasia from hepatic adenoma at gadobenate dimeglumine-enhanced MR imaging: prospective study. Radiology 2005; 236: 166-177.

15. Lubner MG, Smith AD, Sandrasegaran K, et al. CT Texture analysis: definitions, applications, biologic correlates, and challenges. Radiographics 2017; 37: 1483-1503.

16. Li Z, Mao Y, Huang W, et al. Texture-based classification of different single liver lesion based on SPAIR T2W MRI images. BMC Med Imaging 2017; 17: 42. doi: 10.1186/s12880-017-0212-x.

17. Chang CC, Chen HH, Chang YC, et al. Computer-aided diagnosis of liver tumors on computed tomography images. Comput Methods Programs Biomed 2017; 145: 45-51.

18. Sadot E, Simpson AL, Do RK, et al. Cholangiocarcinoma: correlation between molecular profiling and imaging phenotypes. PLoS One 2015; 10: e0132953. doi: 10.1371/journal.pone.0132953.

19. Zhang J, Liu X, Zhang H, et al. Texture analysis based on preoperative magnetic resonance imaging (MRI) and conventional MRI features for predicting the early recurrence of single hepatocellular carcinoma after hepatectomy. Acad Radiol 2019; 26: 1164-1173.

20. Kiryu S, Akai H, Nojima M, et al. Impact of hepatocellular carcinoma heterogeneity on computed tomography as a prognostic indicator. Sci Rep 2017; 7: 12689. doi: 10.1038/s41598-017-12688-7.

21. Chen S, Zhu Y, Liu Z, Liang C. Texture analysis of baseline multiphasic hepatic computed tomography images for the prognosis of single hepatocellular carcinoma after hepatectomy: a retrospective pilot study. Eur J Radiol 2017; 90: 198-204.

Faeze Salahshour, Afshar Ghamari Khameneh, Gisoo Darban Hosseini Amirkhiz, Niloofar Ayoobi Yazdi, Sajad Shafiekhani

22. Thomas JV, Abou Elkassem AM, Ganeshan B, Smith AD. MR imaging texture analysis in the abdomen and pelvis. Magn Reson Imaging Clin N Am 2020; 28: 447-456.

23. Semelka RC, Martin DR, Balci NC. Focal lesions in normal liver. J Gastroenterol Hepatol 2005; 20: 1478-1487.

24. Hectors SJ, Wagner M, Bane O, et al. Quantification of hepatocellular carcinoma heterogeneity with multiparametric magnetic resonance imaging. Sci Rep 2017; 7: 2452. doi: 10.1038/s41598-017-02706-z.

25. Nahm FS. Receiver operating characteristic curve: overview and practical use for clinicians. Korean J Anesthesiol 2022; 75: 25-36.

26. Cannella R, Rangaswamy B, Minervini MI, et al. Value of texture analysis on Gadoxetic acid-enhanced MRI for differentiating hepatocellular adenoma from focal nodular hyperplasia. Am J Roentgenol 2019; 212: 538-546.

27. Zhong X, Tang H, Lu B, et al. Differentiation of small hepatocellular carcinoma from dysplastic nodules in cirrhotic liver: Texture analysis based on MRI improved performance in comparison over Gadoxetic acid-enhanced MR and diffusion-weighted imaging. Front Oncol 2020; 9: 1382. doi: 10.3389/fonc.2019.01382.

28. Stocker D, Marquez HP, Wagner MW, et al. MRI texture analysis for differentiation of malignant and benign hepatocellular tumors in the non-cirrhotic liver. Heliyon 2018; 4: e00987. doi: 10.1016/j.heliyon.2018.e00987.